Acta Crystallographica Section F
Structural Biology and Crystallization Communications
ISSN 1744-3091

Crystallization and preliminary X-ray analysis of human endonuclease 1 (APE1) in complex with an oligonucleotide containing a 5,6-dihydrouracil (DHU) or an α-anomeric 2′-deoxyadenosine (αdA) modified base

Pascal Retailleau,[a,b] Alexander A. Ishchenko,[c] Nikita A. Kuznetsov,[d] Murat Saparbaev[c] and Solange Moréra[a]*

[a]Laboratoire d'Enzymologie et de Biochimie Structurales (LEBS), CNRS, F-91198 Gif-sur-Yvette CEDEX, France, [b]Institut de Chimie des Substances Naturelles (ICSN), CNRS, F-91198 Gif-sur-Yvette CEDEX, France, [c]CNRS UMR 8200 Groupe 'Réparation de l'ADN', Université Paris-Sud, Institut de Cancérologie Gustave Roussy, F-94805 Villejuif CEDEX, France, and [d]Institute of Chemical Biology and Fundamental Medicine, Siberian Branch of the Russian Academy of Sciences, Lavrentyev Avenue 8, Novosibirsk 630090, Russia

Correspondence e-mail: morera@lebs.cnrs-gif.fr

Received 25 March 2010
Accepted 10 May 2010

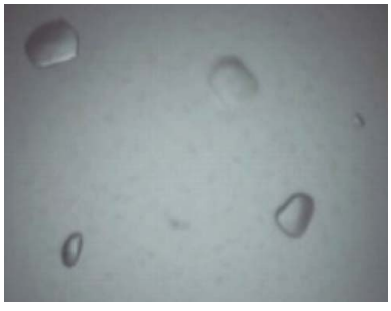

The multifunctional human apurinic/apyrimidinic (AP) endonuclease 1 (APE1) is a key enzyme involved in both the base-excision repair (BER) and nucleotide-incision repair (NIR) pathways. In the NIR pathway, APE1 incises DNA 5′ to a number of oxidatively damaged bases. APE1 was crystallized in the presence of a 15-mer DNA containing an oxidatively damaged base in a single central 5,6-dihydrouracil (DHU)·T or α-anomeric 2′-deoxyadenosine (αdA)·T base pair. Diffraction data sets were collected to 2.2 and 2.7 Å resolution from DNA-DHU–APE1 and DNA-αdA–APE1 crystals, respectively. The crystals were isomorphous and contained one enzyme molecule in the asymmetric unit. Molecular replacement was performed and the initial electron-density maps revealed that in both complexes APE1 had crystallized with a degradation DNA product reduced to a 6-mer, suggesting that NIR and exonuclease reactions occurred prior to crystallization.

1. Introduction

Aerobic respiration and exogenous factors such as ionizing radiation and drugs generate reactive oxygen species (ROS) such as $O_2^{\bullet-}$, H_2O_2, $^{\bullet}OH$ and $NO^{\bullet}$. DNA has limited chemical stability and is one of the most biologically important targets of ROS (Cadet *et al.*, 2003). Oxidative DNA lesions are believed to be a major type of endogenous damage and their accumulation contributes to human degenerative disorders, including cancer, cardiovascular disease and brain dysfunction. The major human apurinic/apyrimidinic (AP) endonuclease (APE1) is a key protein in the repair of oxidative damage to DNA and RNA (Evans *et al.*, 2000; Tell *et al.*, 2010). APE1 participates in both the base-excision repair (BER) and nucleotide-incision repair (NIR) pathways. In the BER pathway, APE1 cleaves DNA at AP sites and 3′-blocking moieties generated by DNA glycosylases (Hitomi *et al.*, 2007). Alternatively, in the NIR pathway APE1 incises 5′ to a damaged base in a DNA glycosylase-independent manner, providing 3′-hydroxy ends for DNA synthesis, coupled with the repair of the remaining 5′-dangling modified nucleotide (Ischenko & Saparbaev, 2002; Gros *et al.*, 2004). APE1 incises DNA containing 5,6-dihydrouracil (DHU) and α-anomeric 2′-deoxyadenosine (αdA) residues, which constitute the major DNA adducts generated by ionizing radiation under anoxic conditions (Jorgensen *et al.*, 1988; Lesiak & Wheeler, 1990; Dizdaroglu *et al.*, 1993). APE1 also possesses a 3′→5′ exonuclease activity which removes 3′-mismatches and oxidized nucleotides (Chou & Cheng, 2002; Parsons *et al.*, 2005) and an endonuclease activity on undamaged DNA which is involved in DNA fragmentation during apoptosis (Yoshida *et al.*, 2003). Interestingly, the NIR and 3′→5′ exonuclease functions of APE1 are genetically linked and are governed by the same amino-acid residues (Daviet *et al.*, 2007; Golan *et al.*, 2010). Previously, we have demonstrated that NIR is a distinct and separable function of AP endonucleases that is essential for handling lethal oxidative DNA lesions which cannot be removed in the BER pathway (Ishchenko *et al.*, 2006).

X-ray structures of apo APE1 have been determined (PDB codes 1bix, 1hd7 and 1e9n; Gorman *et al.*, 1997; Beernink *et al.*, 2001) and

that of APE1 bound to DNA containing a synthetic AP site showed that the enzyme binds to a flipped-out abasic deoxyribose moiety in a pocket that excludes normal DNA nucleotides (Mol *et al.*, 2000). Together with our previous biochemical characterization, these structural data suggest that APE1 may exist in at least two alternative BER-proficient and NIR/exonuclease-proficient conformations in order to accommodate both an abasic site and a damaged base within its active-site pocket.

In order to understand the structural basis of the recognition of a damaged DNA base by an AP endonuclease, we initiated the crystallographic study of APE1 in complex with a DNA fragment containing an oxidatively damaged base as a target base. APE1 was overproduced and purified in an N-terminally truncated form (ΔN61-APE1) since its N-terminal region is known to be highly flexible. Here, we report the crystallization and preliminary X-ray analysis of APE1 in the presence of a DNA fragment containing a damaged base.

2. DNA preparation

The sequence of the 15-mer DNA used for crystallization assays was d(CTGCATA*X*GCATGTA)·d(TACATGCTTATGCAG), where *X* is a damaged base (DHU or αdA). The oligonucleotides were purchased from Eurogentec (Seraing, Belgium) and hybridized by mixing equal concentrations (10 m*M*) in 2 m*M* Tris–HCl pH 7.0 heated to 338 K for 3 min and cooled to room temperature over 2 h. The MALDI–TOF mass-spectrometric analysis of the oligonucleotides performed by the manufacturer validated their size and homogeneity (data not shown). In addition, the purity and integrity of the oligonucleotide preparations were verified by denaturing PAGE (data not shown).

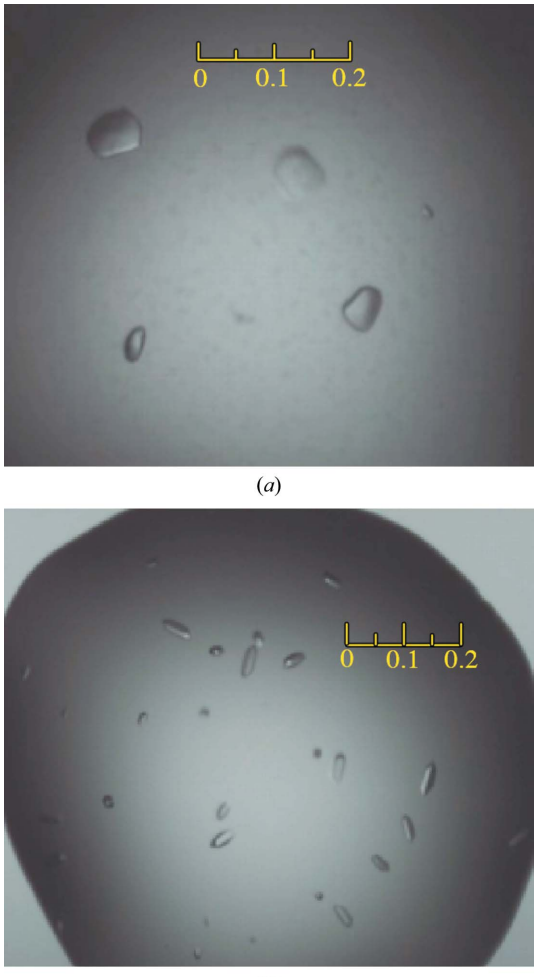

(*a*)

(*b*)

Figure 1
Crystals of DNA-DHU–APE1 (*a*) and DNA-αdA-APE1 (*b*) (the scale bar is labelled in mm).

Table 1
Data-collection statistics.

Values in parentheses are for the highest resolution shell (of nine).

	DNA-DHU–APE1	DNA-αdA–APE1
Space group	$P2_12_12$	$P2_12_12$
Unit-cell parameters (Å)	a = 105.3, b = 44.9, c = 72.4	a = 106.2, b = 45.1, c = 72.6
Resolution (Å)	30.0–2.20 (2.32–2.20)	30.0–2.70 (2.85–2.70)
No. of observed reflections	65369	50675
No. of unique reflections	16482	9659
Completeness (%)	97.6 (97.5)	95.9 (88.0)
$R_{\rm merge}$† (%)	9.3 (40.8)	9.9 (51.2)
$I/\sigma(I)$	6.2 (2.0)	6.8 (2.0)

† $R_{\rm merge} = \sum_{hkl}\sum_i |I_i(hkl) - \langle I(hkl)\rangle| / \sum_{hkl}\sum_i I_i(hkl)$, where $I_i(hkl)$ is the ith observed amplitude of reflection hkl and $\langle I(hkl)\rangle$ is the mean amplitude for all observations i of reflection hkl.

3. Crystallization

ΔN61-APE1 (lacking the first 61 residues) was purified as described by Daviet *et al.* (2007). In crystallization trials, the DNA duplexes were mixed with ΔN61-APE1 protein at a concentration of 7.5 mg ml^{-1} in a buffer consisting of 20 m*M* HEPES pH 7.5 and 130 m*M* KCl in a 2:1 stoichiometry. Commercial crystallization kits (the PEGs II, Classics and MbClass suites from Qiagen) were screened in sitting-drop vapour-diffusion experiments using a nanodrop robot (Cartesian Proteomic Solutions) and 200 nl drops at 293 K. Small crystals appeared within one to two weeks in Classics condition F4 [0.1 *M* HEPES pH 7.5, 10%(*m*/*v*) PEG 8000] and MbClass condition F9 [0.05 *M* sodium phosphate pH 6.8, 12%(*m*/*v*) PEG 4000] for DNA duplexes containing a DHU and an αdA base, respectively (Fig. 1).

4. Data collection and processing

Small crystals were flash-cooled in a cryoprotecting solution consisting of the mother solution supplemented with 25%(*v*/*v*) glycerol. Data-collection experiments were carried out at 100 K on the PROXIMA 1 beamline at SOLEIL (Saint Aubin, France). 150° and 96° of data were collected in 1° frames with 1 s exposure per frame for the DNA-DHU–APE1 and DNA-αdA–APE1 crystals, respectively (Fig. 2). Diffraction intensities were evaluated with the program *XDS* (Kabsch, 2010) to resolutions of 2.2 and 2.7 Å, respectively, and were further processed using the *CCP*4 program suite (Collaborative Computational Project, Number 4, 1994). The crystals of both complexes belonged to the same orthorhombic space group, $P2_12_12$, and are isomorphous. Data-collection and processing statistics are given in Table 1.

5. Molecular replacement

The asymmetric unit can only contain one ΔN61-APE1–DNA complex, corresponding to a Matthews coefficient (Matthews, 1968) of 2.26 Å^3 Da^{-1} and a solvent content of 45.7%. Molecular replace-

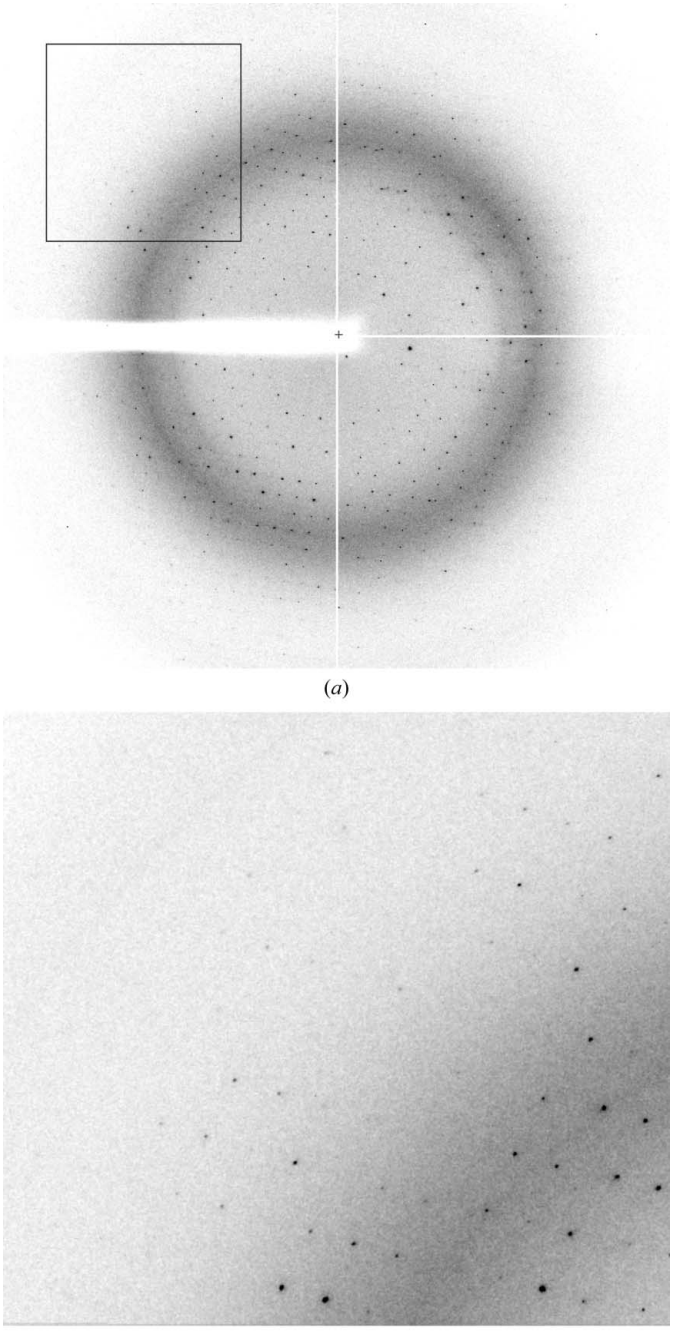

Figure 2
Diffraction pattern of the DNA-DHU–APE1 crystal. (*a*) The outer resolution shell is 2.2 Å (1.7 Å at the edge of the detector). (*b*) Enlarged view of the region marked by a rectangle in (*a*).

ment using the program *Phaser* (Storoni *et al.*, 2004) and the structure of apo APE1 (PDB code 1bix) without the first 61 residues as a search model led to a solution with good scores (RFZ = 18.7 and 17.3, TFZ = 34.5 and 31.5, LLG = 2347 and 1705 for the DNA-DHU–APE1 and DNA-αdA–APE1 crystals, respectively) and an initial *R* factor of 31%. Examination of the resulting model and density maps for both complexes clearly showed that APE1 crystallized with a degraded DNA fragment that was subsequently identified as a 6-mer. One end of the 6-mer enters the active site of APE1, while the opposite end stacks end-to-end in the crystal, forming a pseudo-continuous 12-mer. Refinement of these two APE1 structures in complex with a 6-mer DNA, including attribution of the DNA sequence, is under way.

We are grateful to Andrew Thompson for help in data collection on PROXIMA 1. This work was supported by grants from the Russian Ministry of Education and Science state contract 02.740.11.5012 (to AAI) and MK-1304.2010.4 (to NAK) and from the CNRS GDRE 182, Fondation pour la Recherche Médicale 'EQUIPES FRM 2007' and Electricité de France Contrat Radio-protection RB 2010 (to MS). The crystallization work benefited from the LEBS facilities of the IMAGIF Structural Biology and Proteomic Unit at the Gif campus (http://www.imagif.cnrs.fr).

References

Beernink, P. T., Segelke, B. W., Hadi, M. Z., Erzberger, J. P., Wilson, D. M. III & Rupp, B. (2001). *J. Mol. Biol.* **307**, 1023–1034.
Cadet, J., Douki, T., Gasparutto, D. & Ravanat, J. L. (2003). *Mutat. Res.* **531**, 5–23.
Chou, K.-M. & Cheng, Y.-C. (2002). *Nature (London)*, **415**, 655–659.
Collaborative Computational Project, Number 4 (1994). *Acta Cryst.* D**50**, 760–763.
Daviet, S., Couve-Privat, S., Gros, L., Shinozuka, K., Ide, H., Saparbaev, M. & Ishchenko, A. A. (2007). *DNA Repair*, **6**, 8–18.
Dizdaroglu, M., Laval, J. & Boiteux, S. (1993). *Biochemistry*, **32**, 12105–12111.
Evans, A. R., Limp-Foster, M. & Kelley, M. R. (2000). *Mutat. Res.* **461**, 83–108.
Golan, G., Ishchenko, A. A., Khassenov, B., Shoham, G. & Saparbaev, M. K. (2010). *Mutat. Res.* **685**, 70–79.
Gorman, M. A., Morera, S., Rothwell, D. G., de La Fortelle, E., Mol, C. D., Tainer, J. A., Hickson, I. D. & Freemont, P. S. (1997). *EMBO J.* **16**, 6548–6558.
Gros, L., Ishchenko, A. A., Ide, H., Elder, R. H. & Saparbaev, M. K. (2004). *Nucleic Acids Res.* **32**, 73–81.
Hitomi, K., Iwai, S. & Tainer, J. A. (2007). *DNA Repair*, **6**, 410–428.
Ishchenko, A. A., Deprez, E., Maksimenko, A., Brochon, J. C., Tauc, P. & Saparbaev, M. K. (2006). *Proc. Natl Acad. Sci. USA*, **103**, 2564–2569.
Ischenko, A. A. & Saparbaev, M. K. (2002). *Nature (London)*, **415**, 183–187.
Jorgensen, T. J., Furlong, E. A. & Henner, W. D. (1988). *Radiat. Res.* **114**, 556–566.
Kabsch, W. (2010). *Acta Cryst.* D**66**, 125–132.
Lesiak, K. B. & Wheeler, K. T. (1990). *Radiat. Res.* **121**, 328–337.
Matthews, B. W. (1968). *J. Mol. Biol.* **33**, 491–497.
Mol, C. D., Izumi, T., Mitra, S. & Tainer, J. A. (2000). *Nature (London)*, **403**, 451–456.
Parsons, J. L., Dianova, I. I. & Dianov, G. L. (2005). *Nucleic Acids Res.* **33**, 2204–2209.
Storoni, L. C., McCoy, A. J. & Read, R. J. (2004). *Acta Cryst.* D**60**, 432–438.
Tell, G., Wilson, D. M. III & Lee, C. H. (2010). *Mol. Cell. Biol.* **30**, 366–371.
Yoshida, A., Urasaki, Y., Waltham, M., Bergman, A. C., Pourquier, P., Rothwell, D. G., Inuzuka, M., Weinstein, J. N., Ueda, T., Appella, E., Hickson, I. D. & Pommier, Y. (2003). *J. Biol. Chem.* **278**, 37768–37776.